Optical Engineering

OpticalEngineering.SPIEDigitalLibrary.org

Photosensitive naturally derived resins toward optical 3-D printing

Edvinas Skliutas
Sigita Kasetaite
Linas Jonušauskas
Jolita Ostrauskaite
Mangirdas Malinauskas

SPIE.

Edvinas Skliutas, Sigita Kasetaite, Linas Jonušauskas, Jolita Ostrauskaite, Mangirdas Malinauskas, "Photosensitive naturally derived resins toward optical 3-D printing," *Opt. Eng.* **57**(4), 041412 (2018), doi: 10.1117/1.OE.57.4.041412.

Photosensitive naturally derived resins toward optical 3-D printing

Edvinas Skliutas,[a,*] Sigita Kasetaite,[b] Linas Jonušauskas,[a,c] Jolita Ostrauskaite,[b,*] and Mangirdas Malinauskas[a,*]
[a]Vilnius University, Laser Research Center, Vilnius, Lithuania
[b]Kaunas University of Technology, Department of Polymer Chemistry and Technology, Kaunas, Lithuania
[c]Femtika Ltd., Vilnius, Lithuania

Abstract. Recent advances in material engineering have shown that renewable raw materials, such as plant oils or glycerol, can be applied for synthesis of polymers due to ready availability, inherent biodegradability, limited toxicity, and existence of modifiable functional groups and eventually resulting to a potentially lower cost. After additional chemical modifications (epoxidation, acrylation, double bonds metathesis, etc.), they can be applied in such high-tech areas as stereolithography, which allows fabrication of three-dimensional (3-D) objects. "Autodesk's" 3-D optical printer "Ember" using 405-nm light was implemented for dynamic projection lithography. It enabled straightforward spatio-selective photopolymerization on demand, which allows development of various photosensitive materials. The bio-based resins' photosensitivity was compared to standard "Autodesk" "PR48" and "Formlabs" "Clear" materials. It turned out that the bioresins need a higher energy dose to be cured (a least 16 J · cm^{-2} for a single layer varying from 100 to 130 μm). Despite this, submillimeter range 2.5-D structural features were formed, and their morphology was assessed by optical profilometer and scanning electron microscope. It was revealed that a higher exposition dose (up to 26 J · cm^{-2}) results in a linear increase in the formed structures height, proving controllability of the undergoing process. Overall, the provided results show that naturally derived resins are suitable candidates for tabletop gray-tone lithography. [DOI: 10.1117/1.OE.57.4.041412]

Keywords: photostructurization; dynamic projection lithography; bio-based resin; stereolithography; renewable materials; 3-D printing.

Paper 171569SSP received Oct. 3, 2017; accepted for publication Mar. 13, 2018; published online Apr. 4, 2018.

1 Introduction

In recent decades, new raw materials derived from non-petrochemical feedstock have become an interest for the production of bio-based polymers.[1–3] For example, many biorenewable materials, such as thermosetting resins, thermoplastics, and biocomposites, can be prepared from plant oil-based monomers and their derivatives.[4–6] Recently, glycerol, the byproduct of biodiesel refining, became an important feedstock chemical, which can be used as a monomer in the synthesis of polymers as it is or after chemical modification.[7–9] Heat, pressure,[10] or irradiation by light can be employed to cure prepolymers, including natural oils, by cationic or free radical polymerization.[11] Nowadays, the photoinitiating systems have ever-increasing importance in the industry as these have special significance in many widespread fields, such as optoelectronics and laser imaging, or technologies, such as stereolithography (SLA)[12] and nanotechnology.[13–15] Therefore, there are lots of reports investigating photocuring of various photosensitive systems, mostly of cationic polymerization of epoxides.[16–19]

SLA is relatively straightforward technology practically allowing three-dimensional (3-D) objects formation with low raw material usage.[20] Its precision can reach tens of micrometers in *X*-, *Y*-, and *Z*-axes and speed tens of millimeters per hour in *Z*-axis (we do not emphasize speed in *X*, *Y* plane, because *Z*-axis movement represents total speed of the technology). The technology is based on a layer-by-layer fashion and photopolymerization reaction—a process by which light affects chains of low-molecular mass molecules (monomers or oligomers) and makes link together forming polymers in solid state. In such way, cured micrometer thick range layers then make up the 3-D solid object. The attractiveness and usefulness of potential SLA application (rapid prototyping or low-scale manufacturing of mechanical, medical, optical, or microfluidical devices)[21] allowed this technology to evolve and become commercialized in the form of tabletop devices. Currently, the prices of SLA 3D printing (3DP) can reach a few thousands of Euros, which is acceptable for advanced customers, yet the material price dramatically influences the cost per printed piece. Thus, the wide spread usage of this technology is still limited. To remedy that a lot of attention is directed to improving SLA technology in terms of hardware, firmware, and applicable materials, initial assortment of resins was limited to either only so-called clear resin or its colorful derivatives. They were formulated to deliver the highest-quality output and capture sufficient detail without sacrificing strength. At the same time, in cases of functional printing, objects must have specific mechanical,[22] optical,[23] or biological[24,25] properties. To achieve it, engineering resins, or in other words, functional prototyping materials, were designed. Also, they can simulate and replace a wide range of injection-molded plastics. Objects made out of such materials are characterized by flexibility or durability, resistance for high temperature and even biocompatibility. That highly widens 3DP possibilities and applicability.

One of the most welcome current trends in the field of SLA is open-source manner. It means that device hardware,

*Address all correspondence to: Edvinas Skliutas, E-mail: edvinas.skliutas@ff.vu.lt; Jolita Ostrauskaite, E-mail: jolita.ostrauskaite@ktu.lt; Mangirdas Malinauskas, E-mail: mangirdas.malinauskas@ff.vu.lt

0091-3286/2018/$25.00

firmware, software, electronics, and formulations of the materials are revealed for the public. Users are able to modify listed things by their own requirements as well as share it for the community. It provides a great way to investigate and develop new resins and, therefore, furthering the widening appeal of SLA 3DP.

In this work, we investigate a feasibility for using open-source dynamic light projection (DLP)-based SLA 3DP "Ember" to structure naturally derived resins of glycerol diglycidyl ether (GDGE) and epoxidized linseed oil (ELO). The selective cationic polymerization of such materials achieved via UV lithography and exposition with Ember is shown, and light processing peculiarities are revealed. Achieved results are compared to what is currently available with commercial resin designed for SLA. Overall, we show that photoresins based on renewable biosources are suitable candidates for usage in tabletop SLA 3DP.

2 Materials and Methods

2.1 *Equipment for UV Lithography*

2.1.1 *Thorlabs UV curing LED system CS2010*

"Thorlabs" UV curing LED system "CS2010" (Fig. 1) was used to investigate curing time of bio-based resins. The UV LED power was $P = 270$ mW (corresponding to data sheet), irradiation wavelength $\lambda = 365$ nm, and divergence α from the optical axis 60 deg. The distance D between a sample and LED chip was fixed at 4 cm. An exposed area was calculated by Eq. (1) and was equal to 150 cm^2. Consequently, light intensity I was evaluated by Eq. (2) and was 1.8 mW cm^{-2}

$$S = \pi(D \tan \alpha)^2, \tag{1}$$

$$I = \frac{P}{S}. \tag{2}$$

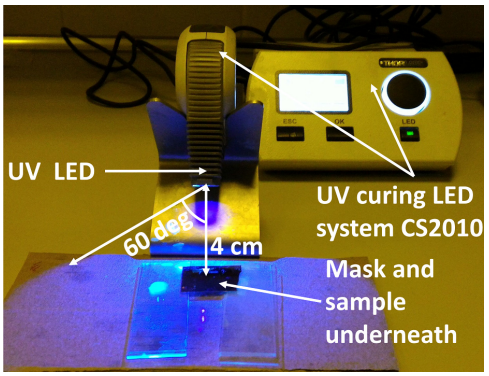

Fig. 1 Thorlabs UV curing LED system CS2010. LED is turned on and exposes 150-cm^2 area (in blue color). There is a sample at the center of the area.

2.1.2 *Autodesk 3-D printer Ember*

"Autodesk's" open-source 3-D optical printer Ember [Fig. 2(a)] was implemented for a dynamic projection lithography (DPL). The light source (projector "Wintech PRO4500") uses 5-W power and 405-nm wavelength, an LED diode, and a digital micromirrors device, which consists of 1280×800 (total 1.024 million) micromirrors spaced in the compact 9855×6161.4 μm^2 footprint. One micromirror pitch size is 7.6 μm, which creates a 50×50 μm^2 projection of a single image pixel, which defines device resolution in X, Y plane. Such an optical system ensures $I = 18.61$ mW cm^{-2} light intensity projected through the UV light transparent polydimethylsiloxane (PDMS) window where the printing process occurs. The intensity is high enough to cure standard resins rapidly. Moreover, it can be modified by changing the electric current flowing through the UV LED. First of all, CAD model is sliced into cross-sectional layers that are transferred to the printer. Then, printing process starts and the images are projected on the PDMS window. The exposed area makes resin to cure one layer at a time and adhere to the build platform or previously formed layers. Single layer height can be from 10 to 100 μm and is controlled by Z-axis stepper and exposure time. The build platform dimensions are 64 mm $\times$ 40 mm $\times$ 134 mm in X-, Y-, and Z-axes. The print preparation software is called "Print Studio," which allows to fix and prepare 3-D files and then delivers them wirelessly to the device. Device working principle is explained in Fig. 2(b).

2.2 *Commercial Resin PR48 and Bio-Based Resins*

Commercial resin Autodesk "PR48" was used as a standard printing material. The resin is acrylate based and mainly consists of methacrylate oligomers and monomers.[26] Exact components are EBECRYL 8210 (Allnex, 39.776% w/w) and SR

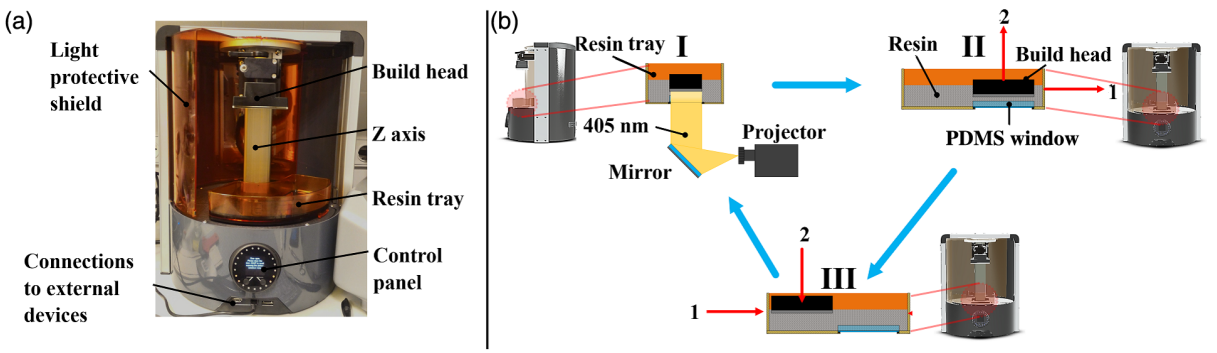

Fig. 2 (a) An open-source 3-D optical printer Ember and (b) its principle working scheme. (I) Irradiation from the projector reflects to the mirror and exposes resin trough the PDMS window, (II) after exposure, the tray slides (1) and the build head rises up, and (III) the tray comes back in it primary position (1) and the build head lowers (2). (I) side view and (II and III) front views.

494 (Sartomer, 39.776% w/w). Being enriched with double bonds, they are suitable for polymerization reaction. Photoinitiator (PI) diphenyl(2,4,6- btrimethylbenzoyl)phosphine oxide (TPO, Esstech, 0.4% w/w) is added to increase photoreactivity. Usually PI used for tabletop SLA makes the resin sensitive to 420-nm wavelength light and lower, with a peak absorption around 365 nm. Also, reactive diluent (RD) plays important role in resin's consist. For example, Genomer 1122 (Rahn, 19.888% w/w) is used to reduce viscosity of the base resin. What is more, RD can react with curing agents to become a part of the polymerization reaction and optimize cured resin's properties, such as impact strength, adhesion, and flexibility.[27] UV blocker 2,2-(2,5-thiophenediyl)bis(5-tertbutylbenzoxazole) (OB, Mayzo, 0.16% w/w) is used in PR48 resin with the purpose to control the light penetration depth, which is needed to confine cured layer thickness. Additionally, various pigments can be mixed up to make resin colorful. However, dye concentration is important, because too much of the pigment makes it to settle out faster. This results in longer exposure time. PR48 initiating system is free radical polymerization proper for a UV lithography.

GDGE (technical grade, Sigma-Aldrich) and ELO (Chemical Point, Germany) were chosen as monomer sources for bio-based resins. Their absorption spectrum is shown in Fig. 3. Both GDGE and ELO can be obtained from some of the cheapest and most abundant nontoxic annually renewable natural resources available in large quantities (in accordance with statistical data, the total production of vegetable oils worldwide amounted to about 177.73 million tons in 2015/2016 year[28] and about 2 million tons of crude glycerol consistently reached the market every year[29]). GDGE and ELO have a high content of reactive functional groups making them suitable components for the preparation of bioresins.[19,30] However, these monomers exhibit low photoreactiveness, and thus efficient PI is mandatory. To cure bio-based resins employing Thorlabs UV Curing LED System CS2010, the following composition was GDGE (or ELO), 3,4-epoxycyclohexylmethyl-3,4-epoxycyclohexane carboxylate (Sigma-Aldrich) as RD, and triarylsulfonium hexafluoroantimonate salts (mixed 50 wt. % in propylene carbonate, Sigma-Aldrich) as PI.

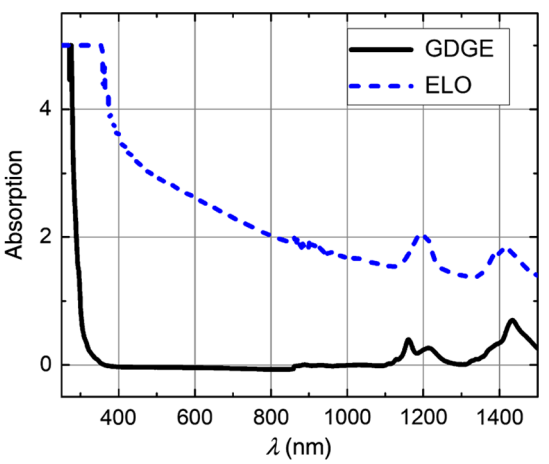

Fig. 3 GDGE and ELO absorption spectrum (λ range from 250 to 1500 nm). ELO absorbs several times more irradiance than GDGE almost in the whole measured range.

Components were mixed accordingly to the weight content of 1 mol. %:30 mol. %:3 mol. %. Polymerization mechanism of such system was mainly cationic since exposure to the UV light of the systems containing no cationic PI did not lead to the appreciable hardening.[27] To cure the resins using Ember, the initiation mechanism was changed to free radical promoted cationic polymerization (FRPCP) following Lalevée protocol,[31] due to the knowledge that the previous PI system was not sensitive to 405-nm wavelength. Chemical compounds were phenylbis(2,4,6-trimethylbenzoyl) phosphine oxide (BAPO, Sigma-Aldrich), diphenyl(2,4,6-trimethylbenzoyl)phosphine oxide (TPO, Rahn) as radical PIs, diphenyl iodonium hexafluorophosphate (Ph_2I^+, Sigma-Aldrich) as a cationic PI, and N-vinylcarbazole (NVK, Sigma-Aldrich) as a promoter. The investigated photoinitiating systems were based on PI/NVK/Ph_2I^+ with weight contents of 3% and 2% for NVK and iodonium salt, respectively.

All composites were mixed by these steps: weighted ingredients, poured into stirring bowl without addition of organic solvent, and stirred with magnetic mixer in the dark for at least 12 h (overnight) until the homogeneous solution was obtained. After it, the composites were ready to use.

2.3 *Other Equipment and Materials*

Thermal power laser measurement sensor "OPHIR 3A-FS" was employed to measure irradiance intensity on the Ember printing area. To evaluate custom-made resins, absorption spectra spectrophotometer "SHIMADZU UVProbe" was implemented. "Q150R" rotary-pumped sputter coater was used to metallize photopolymerized samples as the additional metal layer provides higher conductivity and optical reflectiveness making optical profilometer (OP) and scanning electron microscope (SEM) measurements easier. For characterization, SEM "HITACHI TM-1000" was employed. An OP "SENSOFAR PLμ 2300" was used to obtain formed features profiles and determine their height dependence on absorbed irradiance energy dose.

Isopropyl alcohol was used to leach out noncross-linked monomers from the objects printed out of standard resin PR48. Approximate rinsing time varied from 10 to 15 min. Acetone as a more chemically reactive solvent was implemented to dissolve uncured bio-based resins (rinsing duration 1 to 2 min).

Autodesk "AutoCAD 2017" student version software was employed for CAD models designing.

3 Results

3.1 *Photostructuring Employing CS2010*

Estimated exposure time for commercial resins Autodesk PR48 is a couple of seconds. Ember software Print Studio provides possibility to modify exposure time tuning it to the requirements dictated by any particular material. By default settings, it is set up 1.8 s. However, the first layer is very important for successful fabrication of the whole 3-D object. It must firmly adhere to the building plate, thus longer exposure usually is used (8 s). Naturally derived resins are less sensitive because of long alkyl chains of monomer molecules. For this reason, UV dosages required to polymerize commercial and bio-based resins were compared. Thus, a UV lithography experiment was employed

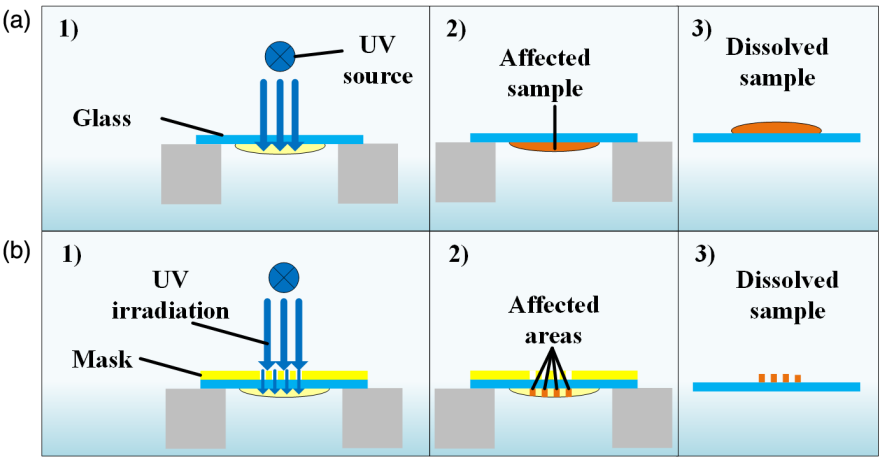

Fig. 4 Resin photocuring scheme: (a) UV lithography: (1) sample droplet exposed to UV ($\lambda = 365$ nm), (2) polymerized droplet, and (3) adhered sample to the substrate after rinsing in acetone. (b) Selective UV lithography: (1) exposition through mask, (2) irradiation affected areas, and (3) dissolved sample, only formed microstructures.

[Fig. 4(a)]. 10-μl droplets of the resins were cast on the 150-μm glass. The hydrophilic interaction between the glass surface and droplets was strong enough to keep the samples upside-down. It ensured adhesion of the formed structure after exposition to the substrate. After exposing the material to UV radiation of 365 nm, the samples were immersed into the solvent (acetone) for 1 min. If the droplets were polymerized, it stayed on the substrate, and if not, it was dissolved. Also, selective UV lithography was performed [Fig. 4(b)]. For this, a micropatterned amplitude mask was used. The mask was the same 150-μm glass slide, coated with 200-nm gold layer. The gold was selectively removed with a femtosecond pulsed laser to form a binary mask (method is described elsewhere).[32] The width of abraded lines was 150 to 400 μm, and the opaque slits between them were 150 μm. After exposing the material to UV radiation through, the mask selective photopolymerization was observed. Acetone dissolved the UV unaffected area, leaving only the formed microstructures.

First, commercial resin PR48 was tested. "Formlabs" "Clear" as additional reference was also investigated. The results showed that both resins are completely polymerized after 2 s of exposure, what corresponds to energy dose $E = 3.6$ mJ cm^{-2}, calculated by Eq. (2) times exposure time. The formed structures are demonstrated in Fig. 5. They consist of single lines, which are strict, defined, thin, and according to the shape of the mask. Keeping the same order, experiments with bio-based resins followed. The exact exposure parameters required to induce photopolymerization reaction in the custom-made resins were unknown. Consequently, the experiment was started with UV lithography to deduce the required dose of irradiation. It was determined that both compositions need to be exposed at least 150 s to UV light (which equals to $E = 270$ mJ cm^{-2}). Exposed droplets of the resins solidified, did not dissolve in acetone, and were easily removable from the substrate. Then, selective UV mask lithography was used. As the mask added additional glass layer, more light was absorbed before affecting the droplets resulting in even longer exposition. For composition with GDGE, time increased to 260 s (468 mJ cm^{-2}), and for composition with ELO, time increased to 220 s (396 mJ cm^{-2}). Despite this, it was possible so obtain selectively polymerized structures (Fig. 6).[33] Compared with objects made from commercial resins, these also had single lines yet with the tendency of merging into the one object. Also, the whole structure was noticeably thicker.

3.2 *Determination of Ember's Spatial Resolution*

Resolution is a very important specification for determining printer's quality. It is defined as a distance among features yet commonly used as a feature size as well. The goal of determining the spatial resolution was to deduce the thinnest separate lines that can be printed using Ember. Thus, a special CAD model was designed (Fig. 7). It consisted of thin vertical walls attached to the base. To determine if there is a

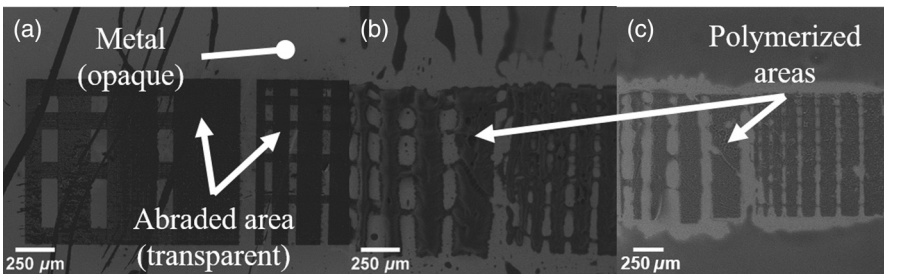

Fig. 5 SEM images: (a) micropatterned amplitude mask. Microstructures after 2-s exposure to UV: (b) Formlabs Clear and (c) Autodesk PR48.

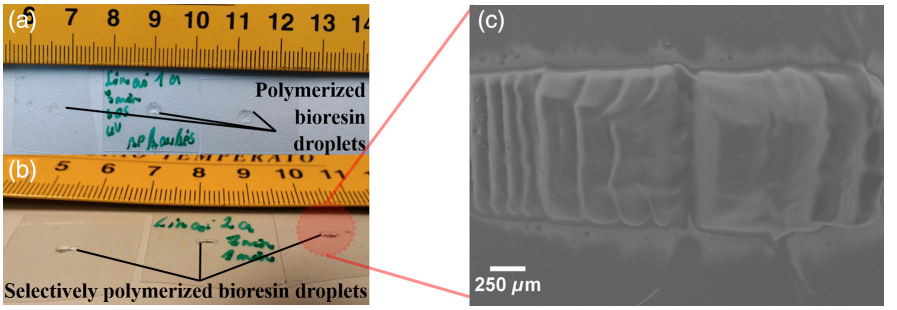

Fig. 6 (a) Polymerized linseed oil-based resin droplets (after 260-s exposure to UV radiation), (b) selectively polymerized droplets (after 220-s exposure to UV radiation), and (c) enlarged view of the droplet (image obtained with SEM).

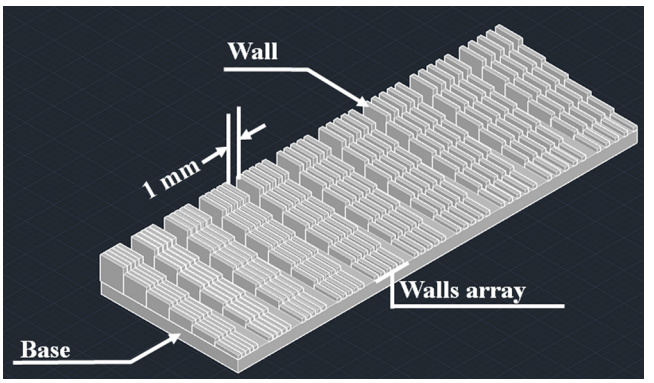

Fig. 7 3-D model of resolution test in "AutoCAD" software.

resolution dependence on the feature aspect ratio, the walls were made of various altitude a, which starts from 0.3 mm (counting from the top of the base) and increases up to 1.5 mm × 0.3 mm step. The highest one was 2 mm. The range of thickness d of the walls was from 50 to 250 μm every 50 μm (total five different models). The slit l between walls varied from 50 to 300 μm every 50 μm. Fixed thick walls with fixed width slits were arranged in arrays. Such arrays were separated from each other with 1-mm gaps. The CAD models were printed with Ember out of standard resin PR48. After manufacturing, the objects were immersed into a solvent. The printed samples were characterized using SEM. Figure 8 shows that the thinnest printed walls were approximately $d = 110$ μm (image a). $l = 200$-μm slit between them was enough to have fully separated walls (image c). Features with a narrower slit between them used to merge to the one object (image b). Compared (a) and (b), it is noticeable that lower features tended to separate from each other better than higher ones with the same slit. It is visible that walls of 0.6-mm height stood apart better than 2-mm ones. It can be explained by overexposure, which occurs during a new layer formation. Light transmits deeper into the previous layers and additionally exposes it. For this reason, the polymerization reaction lasts longer, and the feature spreads wider and merges with the other closest feature. Also, in a similar way, it was deduced that Ember enables printing of 200-μm-diameter circle holes and allows the creation of 250-μm-width rectangular holes.

3.3 *Formation of Woodpile Scaffold Structures*

A lot of results were acquired in collaboration with colleagues from the Institute of Biochemistry, Department of Biological Models (Vilnius University). One of the most frequent tasks was to print 3-D microporous woodpile scaffolds for cell proliferation.[34] Accordingly, it was necessary to investigate if it is possible to manufacture required structures with an available DLP 3DP. The scaffolding microarchitecture models were designed (Fig. 9). Scaffolds' features sizes were set up according to printers' resolution capabilities: $d = 100$ μm, $l = 200$ μm; $d = 200$ μm, $l = 150$ and 200 μm. After fabrication, the objects were postprocessed according the standard protocol. From their SEM images (Fig. 10), it was assessed that structures with 150 μm and narrower slits between

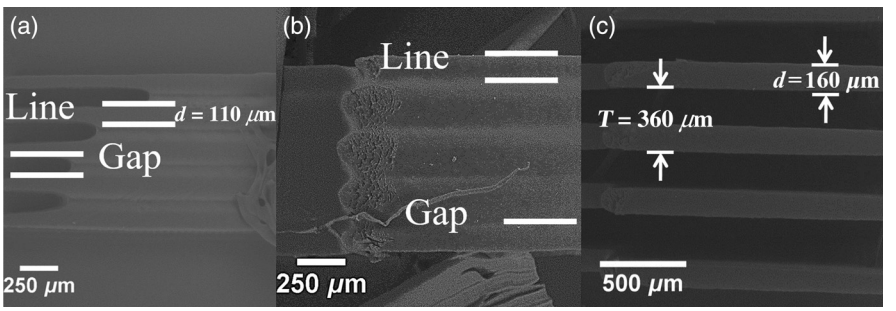

Fig. 8 Ember printed feature size test sample SEM images. d and a represent wall thickness and height, respectively, and l is the distance between walls. (a) $d = 100$ μm, $a = 0.6$ mm, $l = 150$ μm; (b) $d = 100$ μm, $a = 2$ mm, $l = 150$ μm; (c) $d = 150$ μm, $a = 2$ mm, $l = 200$ μm. Compared (a) and (b), higher features tend to merge more than smaller ones. Image (c) shows that features are well separated using more than 150-μm gaps.

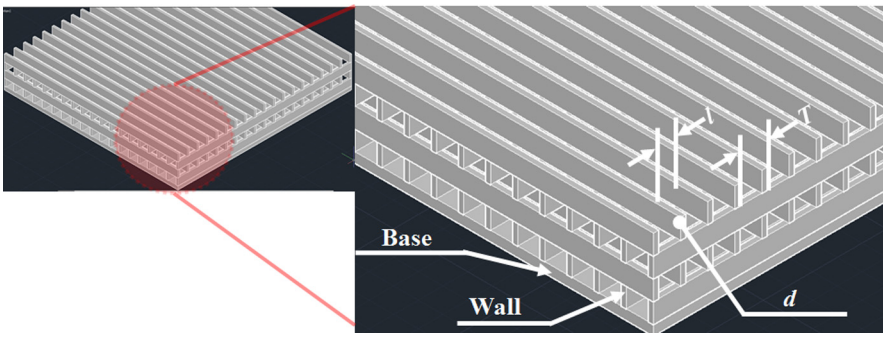

Fig. 9 3-D microporous woodpile scaffold model in AutoCAD software. d is the wall width, l is the gap width, and T is the period ($l + d$).

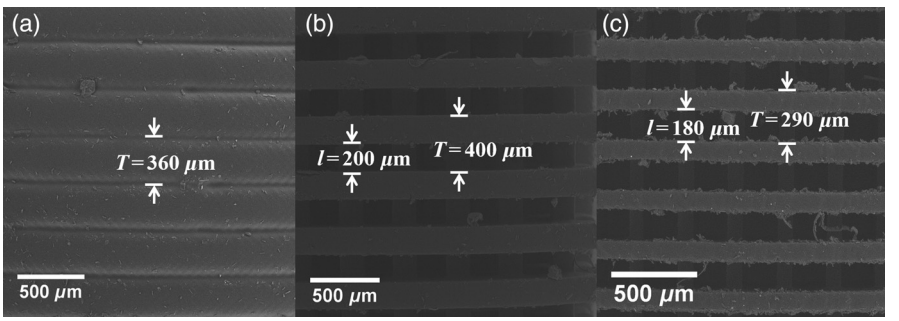

Fig. 10 SEM images of microporous woodpile scaffolds fabricated using Ember. (a) $d = 200$ μm, $l = 150$ μm; (b) $d = 200$ μm, $l = 200$ μm; (c) $d = 100$ μm, $l = 200$ μm.

features were fabricated as one uniform object [Fig. 10(a)]. When l was increased to 200 μm, it was possible to manufacture scaffolds with separated walls [Figs. 10(b) and 10(c)]. Fabricated microporous structures consisted of even 100-μm size features, which is finer to the ones achieved by Jonušauskas et al.[35] The results of cell growing on the 3-D printed scaffolds will be published in a forthcoming publication.[36]

3.4 *Photostructuring of Naturally Derived Resins Employing Ember*

As mentioned before, 405-nm wavelength light source is used in Ember. Using spectrophotometer SHIMADZU UVProbe, it was measured that custom-made resins do not absorb above 375-nm wavelength. Thus, photoinitiating systems were changed from cationic to FRPCP. The system was modified using two different PIs (BAPO and TPO) and varying their weight content from 1% to 5%. The other part of the mixture was GDGE (or ELO) monomers plus 30 mol. % of RD. The concept of the experiment remained the same as photostructuring with CS2010. Glass substrates were used to cast 10-μl droplets on them. The substrates with samples were placed on the PDMS window. Then, selective exposition was turned on. It was projections of special designed CAD model. The model was created corresponding to Ember resolution test results and consisted of 50- to 400-μm-width lines with 50- to 500-μm (both increasing

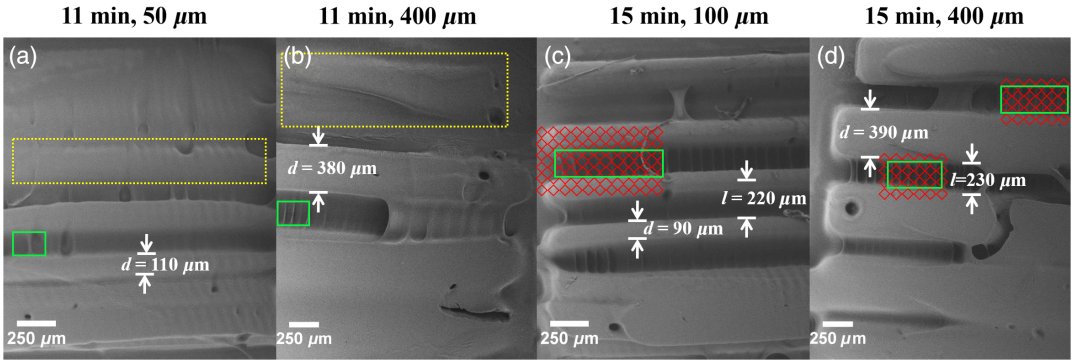

Fig. 11 Selectively polymerized bio-based resin samples and their SEM images: given line width (a) $d = 50$ μm and (b) $d = 400$ μm. Both samples were cured after $E \approx 18$ J cm^{-2}. Yellow dotted rectangles show not fully polymerized lines. (c) $d = 100$ μm and (d) $d = 400$ μm. Cured after $E \approx 24$ J cm^{-2}. Lines were formed more precisely than after shorter exposure. Green rectangles show features, formed perpendicularly to the main lines. In the images (c) and (d), red nets represent pixel arrangement on the PDMS window. Their orientation may cause additional feature formation in the gaps.

every 50 μm)-width slits in between. The light intensity through the PDMS substrate was increased to the maximum and reached 26.54 mW cm^{-2} value. Changing exposure dose selectively, photopolymerized structures were obtained. It was observed that to cure custom-made resins with Ember increased energy dose was required. The best results were obtained when monomers source was GDGE and the initiating system was BAPO/NVK/Ph_2I^+ (3%/3%/2% w/w). In this case, samples were cured after $E \approx 16$ J cm^{-2}. Using less PI (1% and 2%), resulted in dose exceeding 24 J cm^{-2}. Adding more PI (4% and 5%) did not make any significant changes in curing time, showing that inhibition of polymerization started using such high concentrations of PI.[37] When TPO was used instead of BAPO, no samples were photostructurized in 16- to 32-J cm^{-2} energy dose range. After exposure, affected areas looked more transparent than unaffected. However, the samples used to dissolve in acetone leave nothing on the substrate. The same phenomenon was observed with both PIs when ELO was used as a monomer source instead of GDGE.

Table 1 Quality of photostructured various width lines after different energy dose exposure.

	Energy dose (J cm^{-2})		
Lines width (μm)	16 to 18	20	24
50, 100 to 200	Poorly formed lines, barely adhered to the substrate	Well-defined, continuous, and straight lines	
>200	Well-defined, continuous, and straight lines		
Typical height (μm)	100 to 130	190 to 220	250 to 280

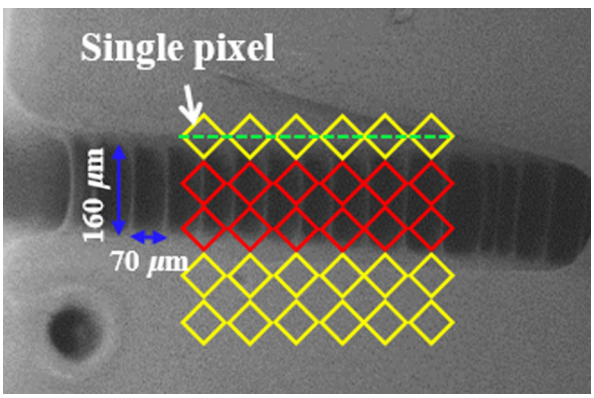

Fig. 12 Enlarged part of the fabricated lines. It shows pixel matrix and its positioning in respect to the lines. Yellow squares represent switched ON pixels and green dashed cursor marks their overlap with line. Blue arrows show scale of the perpendicular stripes.

For further investigations, all obtained samples were sputtered 20-nm gold layer. From SEM images (Fig. 11), it was evaluated that after $E \approx$ 16- to 18-J cm^{-2} lines used to be less ordered, discontinued, prone to be affected by the solvent, shifted, or tilted. 20- to 24-J cm^{-2} exposure ensures well-defined, continuous, and straight lines. Results are summarized in Table 1. Also, wider ones (>200 μm and more) were better adhered to the substrate because of a bigger contact surface area. In all cases, fully separated lines were obtained when a slit in between them was >200 μm. When slit was 100 to 200 μm, it was filled with the leftover of the uncured resin still attached to the produced lines. This made it difficult to distinguish boundaries of the lines. Narrower than 100-μm slits were totally filled with uncured material or clogged up. What is more, small circular "craters" can be noticeable on the formed features (see Figs. 11 and 12). They were caused by air microbubbles that appeared when sample droplets were casted on the glass substrate. However, this issue can be solved putting droplets in vacuum. After several iteration of vacuuming, no bubbles were seen in hand-spread droplets. Microbubbles should not be a problem for layer-by-layer SLA 3DP, due to translation of build head, which pushes out all the bubbles in the resin as it is in standard use of commercial materials. Also, small stripes were noticeable in the slits oriented perpendicular to the main lines similar to repolymerization at nanoscale as explained in other reports.[38] They most likely appeared due to diagonal pixel matrix orientation to the PDMS window. Figure 12 demonstrates how perpendicular stripes could be formed. Red-yellow squares net represents pixel matrix with yellow ones symbolizing ON state pixels (which expose the material) and red symbolizing OFF state. As it is shown, only half of upper yellow squares overlap with the line (marked with a green cursor). In such case, allegedly, the pixels turn to ON state and illuminate additional area, which normally should not be exposed. The same happens with pixels overlapping with other lines. Stripes were periodically arranged and their locations

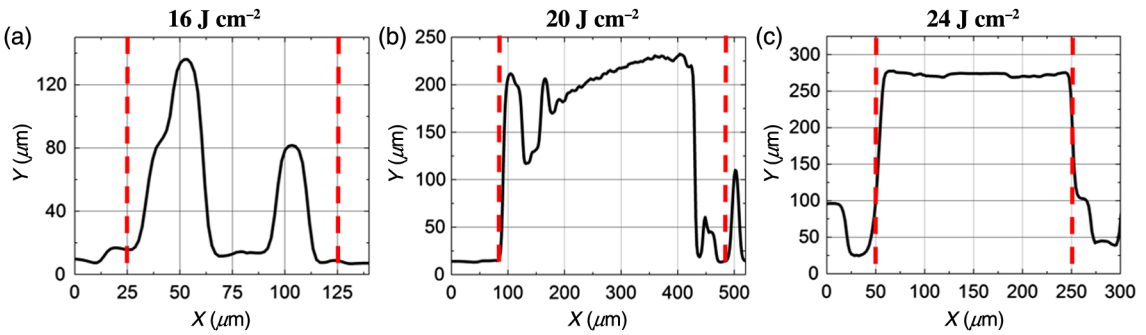

Fig. 13 Measured formed lines cross sections. Exposure dose, measured (and given) width, and height: (a) $E \approx 16$ J cm^{-2}, $d = 88(100)$ μm, $a = 121$ μm; (b) $E \approx 20$ J cm^{-2}, $d = 365(400)$ μm, $a = 201$ μm; (c) $E \approx 24$ J cm^{-2}, $d = 219(200)$ μm, $a = 252$ μm. Red dashed cursors mark given width.

coincided with pixels positioning. Distance between those stripes varied from 65 to 75 μm, which correlates with square hypotenuse ($\approx$70.7 μm). In our predictions, such a device working principle explains perpendicular stripes origin and narrow slits clogging. Varying and achieving optimal printable objects orientation in respect to the pixels alignment, it might be possible to achieve higher resolution.

Furthermore, the cross sections of formed lines were obtained with an OP (Fig. 13). It allowed evaluation of their height depending on absorbed energy dose. It was assessed that after lower doses lines had less height, compared to those, which absorbed more energy. Usually, 100- to 130-μm height lines were photostructurized after $E \approx$ 16 to 18 J cm^{-2}, 190 to 220 μm after $E \approx 20$ J cm^{-2} and 250 to 280 μm after $E \approx 24$ J cm^{-2}. It shows that more irradiance is absorbed, and more material is polymerized. From sections picture, it is noticeable that thinner lines were formed less accurately than wider ones.

4 Discussion

The prospect of bioresins that can be structured via light in a spatio-selective manner is important for many reasons. First of all, being made from renewable sources, they should be cheap, easily obtainable, and biocompatible. Later, quality makes them suitable for home use, medicine, and simplified disposal of objects created out of them. Also, this correlates well with the fast growth of 3DP technologies, especially SLA-based ones. Open sourcing of the 3DP brings a great value in development of new photocurable materials.[39] Combining the aforementioned two should lead to creation of structures that could be applicable in many different science fields, such as microfluidics,[40] optics, and biomedicine. In our work, we showed that bioresins, based on naturally derived monomers, can be selectively photostructurized employing both UV lithography (365 nm) and DPL (which uses practically visible light—405 nm). Depending on photoinitiating system (cationic or FRPCP), it is possible to adjust materials cross-linking rate and photosensitivity to a certain wavelength. We investigated that the bioresins are an appropriate medium to reach hundreds of micrometers in spatial resolution. There were successfully structured 100-μm-width lines with 200-μm slits between them. Significant results are that lines height can be controlled by exposed irradiation dosage. We evaluated that in the 16- to 26-J cm^{-2} range it is possible to modify features height in several hundreds micrometers range. The results show that renewable biosources can be used in SLA 3DP as new resins for rapid prototyping. However, it is still directly difficult to compare the custom-made resins with commercially available ones. Comparative properties can be distinguished in sense of printing properties (photoreactivity,[19] viscosity,[41] layer thickness, and resolution) and ones of printed objects (mechanical[42] and chemical characteristics[43]). The presented photoinitiating systems require higher energy doses, resulting in prolonged exposure times. Thus, additional chemical modifications, more powerful light sources, other photoinitiating systems, or monomers sources could be an option for achieving more practical results. For example, Miao et al.[44] showed photostructuring of photosensitized acrylated epoxidized soybean oil based on free radical photopolymerization (as usual in optical 3DP), and Voet et al.[41] demonstrated successful fabrication of complex shaped prototypes structures from bio-based acrylate photopolymer resins, employing tabletop SLA. Such resins would have a significant advantage because of their easy production, environmental friendship, and relatively low price. Furthermore, they can be applied for 3-D optical structuring down to nanoscale by employing ultrafast lasers.[45]

5 Conclusions

In this work, a tabletop open-source 3-D optical printer Ember was evaluated and its spatial resolution was determined. It was assessed that the device is capable of forming 3-D structures having internal microarchitecture with feature sizes in the hundreds micrometers range. Furthermore, naturally derived monomer-based resins were presented in this paper. Cationic and free radical promoted cationic photoinitiating systems employing UV lithography and DPL were investigated. Custom-made resins photoreactivity was compared with standard ones. It was evaluated that bio-based resins are less photoreactive and require higher energy doses to cure. Despite this, we showed that it is possible to implement selective photopolymerization in it and to control formed features sizes varying irradiation dosage.

The development of practical visible light PI systems for the rapid photopolymerization of naturally derived monomers makes it possible to consider these systems for wide use in many applications. The results show their great perspectives to be applied in UV lithography field for 2.5-D structure formation or even in the 3DP.

Acknowledgments

The financial support from the Research Council of Lithuania (No. S-LAT-17-2) is gratefully acknowledged. Mr. Mindaugas Motiejūnas (Biolabas) is acknowledged for sharing initiative toward 3DP of renewable bioresins. The authors declare no conflict of interest.

References

1. T. F. Garrison, A. Murawski, and R. L. Quirino, "Bio-based polymers with potential for biodegradability," *Polymers* **8**(7), 1–22 (2016).
2. L. Fertier et al., "The use of renewable feedstock in UV-curable materials—a new age for polymers and green chemistry," *Prog. Polym. Sci.* **38**(6), 932–962 (2013).
3. U. Biermann et al., "Oils and fats as renewable raw materials in chemistry," *Angew. Chem. Int. Ed.* **50**(17), 3854–3871 (2011).
4. C. Zhang et al., "Recent advances in vegetable oil-based polymers and their composites," *Prog. Polym. Sci.* **71**, 91–143 (2017).
5. G. Lligadas et al., "Renewable polymeric materials from vegetable oils: a perspective," *Mater. Today* **16**(9), 337–343 (2013).
6. S. Miao et al., "Vegetable-oil-based polymers as future polymeric biomaterials," *Acta Biomater.* **10**(4), 1692–1704 (2014).
7. A. Hejna et al., "Potential applications of crude glycerol in polymer technology—current state and perspectives," *Renew. Sustainable Energy Rev.* **66**, 449–475 (2016).
8. P. D. Pham et al., "Various radical polymerizations of glycerol-based monomers," *Eur. J. Lipid Sci. Technol.* **115**(1), 28–40 (2013).
9. A. Behr and J. P. Gomes, "The refinement of renewable resources: new important derivatives of fatty acids and glycerol," *Eur. J. Lipid. Sci. Technol.* **112**(1), 31–50 (2010).
10. H. Chen, Z. Zhang, and Q. Gao, "PMMA micro-pillar forming in micro channel by hot embossing," *Int. Polym. Proc.* **31**(3), 364–368 (2016).
11. V. Sharma and P. P. Kundu, "Addition polymers from natural oils—a review," *Prog. Polym. Sci.* **31**(11), 983–1008 (2006).
12. X. Chen et al., "Experimental design and parameter optimization for laser three-dimensional (3-D) printing," *Lasers Eng.* **33**(1–3), 189–196 (2016).
13. Y. Yagci, S. Jockusch, and N. J. Turro, "Photoinitiated polymerization: advances, challenges, and opportunities," *Macromolecules* **43**(15), 6245–6260 (2010).
14. H.-B. Sun and S. Kawata, "Two-photon photopolymerization and 3D lithographic microfabrication," in *NMR 3D Analysis Photopolymerization*

(Advances in Polymer Science), pp. 169–273, Springer, Berlin, Heidelberg (2004).
15. C. Barner-Kowollik et al., "3D laser micro- and nano-printing: challenges for chemistry," *Angew. Chem. Int. Ed.* **56**(50), 15828–15845 (2017).
16. J. V. Crivello, T. Yoo, and J. A. Dougherty, "Synthesis and cationic photopolymerization of alkoxyallene monomers," *J. Polym. Sci. Part A: Polym. Chem.* **33**(14), 2493–2504 (1995).
17. J. L. Stanford, A. J. Ryan, and Y. Yang, "Photoinitiated cationic polymerization of epoxides," *Polym. Int.* **50**(9), 986–997 (2001).
18. Z. Zong, J. He, and M. D. Soucek, "UV-curable organic–inorganic hybrid films based on epoxynorbornene linseed oils," *Prog. Org. Coat.* **53**(2), 83–90 (2005).
19. A. Remeikytė, J. Ostrauskaitė, and V. Gražulevičienė, "Synthesis and properties of photocross-linked polymers of epoxidized linseed oil with different reactive diluents," *J. Appl. Polym. Sci.* **129**(3), 1290–1298 (2013).
20. F. P. W. Melchels, J. Feijen, and D. W. Grijpma, "A review on stereolithography and its applications in biomedical engineering," *Biomaterials* **31**(24), 6121–6130 (2010).
21. N. Bhattacharjee et al., "The upcoming 3D-printing revolution in microfluidics," *Lab. Chip.* **16**(10), 1720–1742 (2016).
22. J. Stampfl et al., "Photopolymers with tunable mechanical properties processed by laser-based high-resolution stereolithography," *J. Micromech. Microeng.* **18**(12), 125014 (2008).
23. K. D. D. Willis et al., "Printed optics: 3D printing of embedded optical elements for interactive devices," in *Proc. of the 25th Annual ACM Symp. on User Interface Software and Technology*, pp. 589–598 (2012).
24. M. N. Cooke et al., "Use of stereolithography to manufacture critical-sized 3D biodegradable scaffolds for bone ingrowth," *J. Biomed. Mater. Res. Part B Appl. Biomater.* **64**(2), 65–69 (2003).
25. F. Yanagawa, S. Sugiura, and T. Kanamori, "Hydrogel microfabrication technology toward three dimensional tissue engineering," *Regener. Ther.* **3**, 45–57 (2016).
26. H. Gong et al., "Optical approach to resin formulation for 3D printed microfluidics," *RSC Adv.* **5**(129), 106621–106632 (2015).
27. E. A. C. Demengeot et al., "Crosslinking of epoxidized natural oils with diepoxy reactive diluents," *J. Appl. Polym. Sci.* **115**, 2028–2038 (2010).
28. "Production of major vegetable oils worldwide from 2012/13 to 2016/2017, by type (in million metric tons)," https://www.statista.com/statistics/263933/production-of-vegetable-oils-worldwide-since-2000/ (15 September 2017).
29. R. Ciriminna et al., "Understanding the glycerol market," *Eur. J. Lipid Sci. Technol.* **116**, 1432–1439 (2014).
30. S. Kašėtaitė et al., "Photocross-linking of glycerol diglycidyl ether with reactive diluents," *Polym. Bull.* **72**(12), 3191–3208 (2015).
31. J. Lalevée et al., "N-Vinylcarbazole: an additive for free radical promoted cationic polymerization upon visible light," *ACS Macro Lett.* **1**(7), 802–806 (2012).
32. S. Butkus et al., "Analysis of the micromachining process of dielectric and metallic substrates immersed in water with femtosecond pulses," *Micromachines* **6**(12), 2010–2022 (2015).
33. E. Skliutas et al., "Bioresists from renewable resources as sustainable photoresins for 3D laser microlithography: material synthesis, cross-linking rate and characterization of the structures," *Proc. SPIE* **10115**, 1011514 (2017).
34. M. Malinauskas et al., "3D microporous scaffolds manufactured via combination of fused filament fabrication and direct laser writing ablation," *Micromachines* **5**(4), 839–858 (2014).
35. L. Jonušauskas et al., "Custom on demand 3D printing of functional microstructures," *Lith. J. Phys.* **55**(3), 227–236 (2015).
36. G. Grigalevičiūtė et al., "Fabrication of flexible microporous 3D scaffolds via stereolithography and optimization of their biocompatibility," *Proc. SPIE* **10544**, 105441E (2018).
37. S. Dadashi-Silab, S. Doran, and Y. Yagci, "Photoinduced electron transfer reactions for macromolecular syntheses," *Chem. Rev.* **116**(17), 10212–10275 (2016).
38. M. Malinauskas et al., "Self-polymerization of nano-fibres and nano-membranes induced by two-photon absorption," *Lith. J. Phys.* **50**(1), 135–140 (2010).
39. S. H. Pyo et al., "Continuous optical 3D printing of green aliphatic polyurethanes," *ACS Appl. Mater. Interfaces* **9**(1), 836–844 (2016).
40. X. Chen et al., "Manufacturing methods and applications of membranes in microfluidics," *Biomed. Microdevices* **18**(6), 1–13 (2016).
41. V. S. D. Voet et al., "Biobased acrylate photocurable resin formulation for stereolithography 3D printing," *ACS Omega* **3**(2), 1403–1408 (2018).
42. B. Steyrer et al., "Visible light photoinitiator for 3D-printing of tough methacrylated resins," *Materials* **10**(12), 1445 (2017).
43. F. Kotz et al., "Highly fluorinated methacrylates for 3D printing of microfluidic devices," *Micromachines* **9**(3), 115 (2018).
44. S. Miao et al., "4D printing smart biomedical scaffolds with novel soybean oil epoxidized acrylate," *Sci. Rep.* **6**(1), 27226 (2016).
45. M. Malinauskas et al., "Ultrafast laser processing of materials: from science to industry," *Light. Sci. Appl.* **5**(8), e16133 (2016).

Edvinas Skliutas currently is an engineer at the Laser Research Center. He received his BS degree in applied physics from Vilnius University in 2017 and continues his studies on MS, specialized in laser technology. His research interests include optical three-dimensional (3-D) printing, UV lithography, two-photon polymerization, 3-D microporous scaffolds fabrication, and photosensitive naturally derived resin development. He is an officer of the SPIE Vilnius University Chapter and the OSA Student Chapter of Vilnius University

Sigita Kasetaite received her bachelor's degree in chemistry in 2012 and her master's degree in chemical engineering from Kaunas University of Technology in 2014. Currently, she is a PhD student of chemical engineering at Kaunas University of Technology. Her main scientific interests include modification of naturally occurring materials, synthesis of bio-based polymers, and investigation of their properties.

Linas Jonušauskas received his bachelor's degree as a physicist from Vilnius University, Faculty of Physics in 2014. Currently, he is working toward his master's degree. His main scientific interests include fabrication of various functional microdevices using direct laser writing lithography and its fabrication optimization.

Jolita Ostrauskaite received her master's degree in polymer chemistry from Kaunas University of Technology in 1993. She obtained her PhD from the Department of Organic Technology, Kaunas University of Technology in 2002. Her main scientific interests include synthesis, modification, and investigation of bio-based polymers, biodegradable polymers, and biocomposites, and synthesis and properties of organic electronically active low-molar-mass and polymeric compounds.

Mangirdas Malinauskas received his bachelor's and master's degree as a physicist from Vilnius University in 2006. He obtained his PhD from the Department of Quantum Electronics in 2010. During his career, he has made traineeships in LZH (Hannover) and IESL FORTH (Heraklion). Currently, he continues investigation on ultrafast laser 3-D additive and subtractive structuring of polymers and its combination with alternative lithographic techniques for potential applications in micro-optics, photonics, cell studies, and biomedicine at the Laser Research Center, Vilnius University.